Optimized Heat Pump Design for GCC countries, Part I: Algorithm

H. Javed, O. A. Qureshi, M. T. Ali, P. R. Armstrong
Masdar Institute of Science and Technology

Abstract:
A general component-based model of an air-cooled chiller is developed to be used as the analysis tool for optimal design of GCC specific cooling equipment. Each component is modeled from first principles and/or empirical relations selected to be valid over a wide range of operating conditions, speed and load. The components include a two stage economized screw compressor, shell-and-tube evaporator and air cooled finned tube condenser with R134a as refrigerant. The component-based model predicts COP of a particular design given cooling load and conditions. A performance map generated by the plant model is embedded in the objective function of an optimization problem that determines the optimal sub-cooling for any load and operating condition by grid search method. The resulting annual savings for optimal subcooling control design is estimated to be 1.7% for Abu Dhabi

Key Words: Heat Pump, Baseline Chiller, Optimal Control, GCC-specific equipment.

1 INTRODUCTION AND LITERATURE REVIEW

The United Arab Emirates (UAE) experience hot and humid weather conditions for most months of the year. Cooling represents 40-55% of annual electricity consumption and during peak summer days, cooling systems consume 60-75% of electrical energy (Ali 2011; Friedrich 2013). The gross cost to generate electricity with domestic oil and gas is estimated to be 0.12USD/kWh (Husseini et al. 2008).

Heat pump products, like other energy-intensive capital equipment, compete in the market on both first cost (price) and operating cost defined in terms of *climate specific* Seasonal Energy Efficiency Rating (SEER). Although life-cycle cost (LCC) may be estimated and considered by some, the average buyer is influenced more by first cost. To reduce the impact of this irrational behavior and simultaneously transform markets toward higher fleet efficiency, many countries adopt minimum performance standards for heat pump equipment. The efficiency bar generally aims to minimize LCC of a given machine type and size category serving a typical load profile.

This paper describes a component-based model for an air cooled roof top chiller selected as the baseline chiller from which to develop optimal GCC-specific equipment designs for machines in the 200 to 1000kW range. Each chiller plant component is modeled from first principles and/or empirical relations known to be valid over a wide range of conditions, flow rate and load. The component-based cooling plant model of Zakula (2012) is scaled and adapted to model the baseline chiller and produce tabular performance maps. The cooling plant model may be used to assess different compressor types and staging arrangements, to determine optimal condenser and evaporator size for a given rated chiller capacity, and to determine optimal combination of compressor, condenser and evaporator fan/pump speeds and condenser sub-cooling for any load and operating condition. Data source, heat balance analysis and instrumentation for verification of this baseline model are presented in companion paper (M.T.Ali 2014).

Heat pump and component models for chiller plants are extensively described in the literature. Complex and computationally expensive models which require a large number of input variables are commonly used by manufactures for design purposes. Zakula et al (2011), Hiller (1976), Ellison et al (1979) and Rice (2006) describe comprehensive air-to-air Heat Pump Models (HPMs), where the reported error for output of interest such as COP and

capacity is within 5%. Because market competition makes producers reluctant to publish chiller design and performance parameters, researchers have developed simple component models derived from first principles or empirical relations. Braun et al (1987) developed a simple mechanistic model to predict performance of a chiller plant and compared the results with supervisory control and data acquisition (SCADA) values, under both constant and variable speed control. Van Houte et al (1994), Jin (2002), and Vera-García et al (2010) also presented various simple component models based on physics and semi-empirical relations. Armstrong et al (2009) presented a set of coupled first principles component models to optimize compressor and fan speeds for minimal total power given cooling rate, zone and ambient temperature. This work was further developed by Zakula et al (2011) by taking into account refrigerant-side pressure drops, suction superheat, condenser sub-cooling and variable heat transfer coefficients. Use of variable- instead of fixed-speed compressors can save 25-35% according to Cohen et al (1974) and Qureshi (2013). These savings result from reduced condenser pressure and increased evaporator pressure at part load.

2 HEAT PUMP MODEL FORMULATION

The heat pump model consists of three component models within a main solver. Evaporator, condenser and compressor parameters are determined by regression using first principles models wherever possible. Trial values are assumed for evaporator inlet enthalpy and compressor discharge pressure. Refrigerant mass flow rate, evaporator saturated pressure and temperature, and chilled water supply are the outputs from the evaporator sub-model given cooling load, chilled water return temperature, mass flow rate of chilled water, degree of superheat and trial refrigerant inlet enthalpy. Refrigerant mass flow rate and pressure ratio are input to the compressor isentropic efficiency model, which returns compressor power and discharge temperature. Similarly, given the mass flow rates and inlet temperatures from air- and refrigerant-sides, the condenser model provides rejected heat rate, condenser pressure, and temperature of the leaving refrigerant liquid. The solver has converged when the calculated condenser pressure and liquid temperature at condenser outlet match latest trial values of pressure and temperature to a given tolerance.

2.1 Compressor

The compressor model uses two sub models to compute refrigerant flow rate and input power given compressor speed and pressure ratio. These models are based on the fact that leakage, flow losses, and internal power dissipation are more-or-less proportional to refrigerant flow rate and compressor work with an additional loss component proportional to departure from the built-in volume index. Thus we can use 1st or 2nd order models to empirically represent deviations from the idealized models of flow proportional to speed and constant isentropic efficiency. These low-order models can be used over the range of pressure ratio and mass flow rate encountered in chiller operation. Model outputs include compressor input power, compressor discharge temperature and compressor speed. Intermediate variable of isentropic efficiency is also determined.

2.1.1 Capacity Model.

A relation is needed between compressor speed and mass flow rate. Here we model inlet port flow per stroke ($\dot{V}_{ref}/f$) as a bi-quadratic relation in compressor speed (f) and pressure ratio (π), shown in figure1.

$$\dot{V}_{ref} / f = function(\pi, f)$$

where

$$\dot{V}_{ref} = \dot{m}_{ref} / \rho_{in}$$

The model is trained and verified for selected chiller data points from April-March, 2014. The refrigerant mass flow rate, $\dot{m}_{ref}$, is inferred from the evaporator heat balance using continuously measured chilled water flow rate and chilled water temperatures (return and supply) as well as entering and leaving refrigerant specific enthalpy. The regression coefficients and t-statistics (ASHRAE Guide-2 2005) of the capacity model are presented in Table 1. When the relation is inverted to predict compressor speed given refrigerant flow rate and pressure ratio, the prediction, shown in Figure 3(b) is within ±5% of measured for compressor speed above 100 Hz. Relatively little data is available for operation below 100 Hz because the plant is designed to go beyond 2:1 capacity turndown by sequentially adding compressors. The model is considered less reliable in this region because of transient effects and relative lack of data below 100Hz compressor speed.

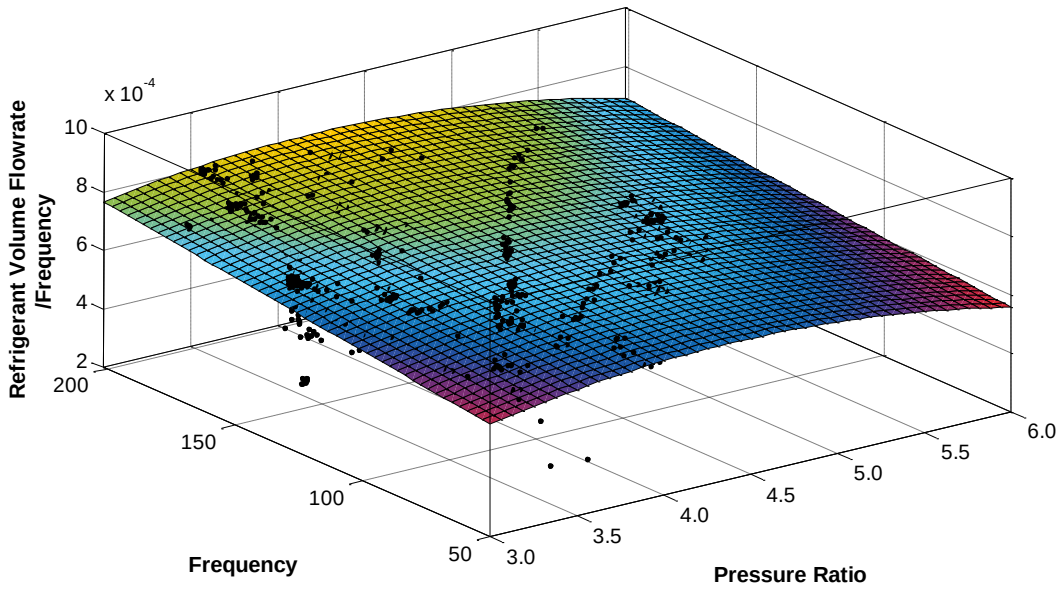

Figure 1 : Capacity Model Map

Coefficient	Term	Value	t-stat
C_1	Constant	-2.094E-04	-1.004
C_2	π	3.694E-04	4.161
C_3	f	1.507E-06	1.470
C_4	π^2	-4.153E-05	-3.863
C_5	$\pi . f$	-1.009E-07	-0.449
C_6	f^2	0.000	0.000

Table 1 : Bi-quadratic relation for $\dot{V}_{ref}/f$ producing RMS = 8.997e-05 for points shown in Figure 1

2.1.2 Isentropic Efficiency Model.

Isentropic efficiency is a measure of how closely the actual compression process approaches the reversible compression process between inlet and discharge pressures. The discharge temperature is always higher in the actual than for the reversible process and this temperature difference represents energy that is dissipated as I^2R, mechanical friction, flow, and abrupt expansion losses in the compressor. The definition of isentropic efficiency (Stoecker 1982) is

$$\eta_{isen} = \frac{h_{is} - h_{in}}{h_{out,a} - h_{in}}$$

where $h_{is} = h_{vapor}(P_{dis}, S_{in})$ is the discharge enthalpy for a reversible compression process.

To characterize compressor performance over wide range of operating conditions we take isentropic efficiency to be a function of pressure ratio and compressor speed (Brasz 2010):

$$\eta_{isen} = function(\pi, f)$$

A bi-quadratic relation (Qureshi 2014) was trained to selected (i.e. near steady state) chiller data points from April-March 2014. Isentropic efficiency is predicted within four percentage points (standard error) of measured isentropic efficiency; resulting isentropic efficiency is plotted against range of pressure ratios and compressor speed, shown in Figure 2. The behavior differs from the semi-empirical results presented for a reciprocating compressor in Armstrong et al (2009) because the M1A compressor is a screw compressor in which losses significantly above or below the design volume ratio are dominated by abrupt expansions at the discharge port. Reciprocating compressor losses are more dominated by friction and flow losses which increase monotonically with compressor speed.

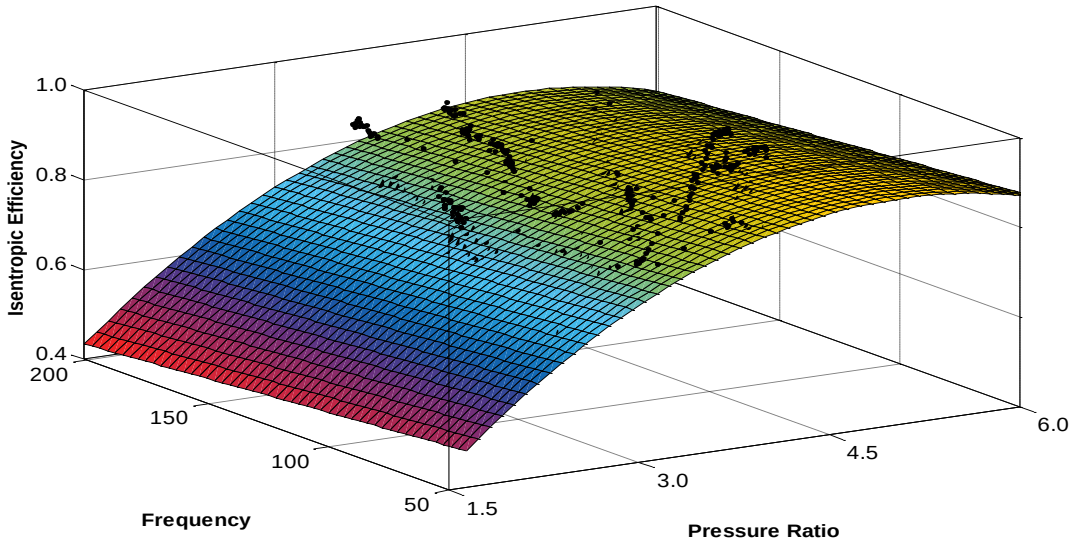

Figure 2 : Isentropic Efficiency Map for range of Pressure ratios and compressor speed

Coefficient	Term	Value	t-stat
C_1	Constant	7.054E-02	0.711
C_2	π	3.539E-01	8.383
C_3	f	-4.312E-04	-0.885
C_4	π^2	-3.596E-02	-7.034
C_5	$\pi . f$	0.000	0.000
C_6	f^2	0.000	0.000

Table 2 : Bi-quadratic relation for η_{isen} producing RMS = 0.04275 for points shown in Figure 2

The foregoing bi-quadratic regression models are of the form

$$y = \sum_i C_i f_i(\bar{X}) + \varepsilon$$

where, y is the volumetric flow rate ($\dot{V}_{ref}$) or isentropic efficiency η_{isen}, $\bar{X} = [f, \pi]$ is the vector of independent variables, $f_i(\bar{X})$ is the i^{th} bi-quadratic term, C_i is the regression coefficient associated with $f_i(X)$ and ε is the error or residual.
To evaluate the compressor model outlet enthalpy $h_{out,a}$ is evaluated from isentropic efficiency relation described previously, where $h_{is} and\ h_{in}$ are respective enthalpies.

$$h_{out,a} = h_{in} + \frac{h_{is} - h_{in}}{\eta_{isen}}$$

Compressor work can then be calculated as follows

$$\dot{W} = \dot{m}_{ref}\left(h_{out,a} - h_{in}\right)$$

Compressor power is predicted by this procedure within ±10%, as shown in figure 3(a)

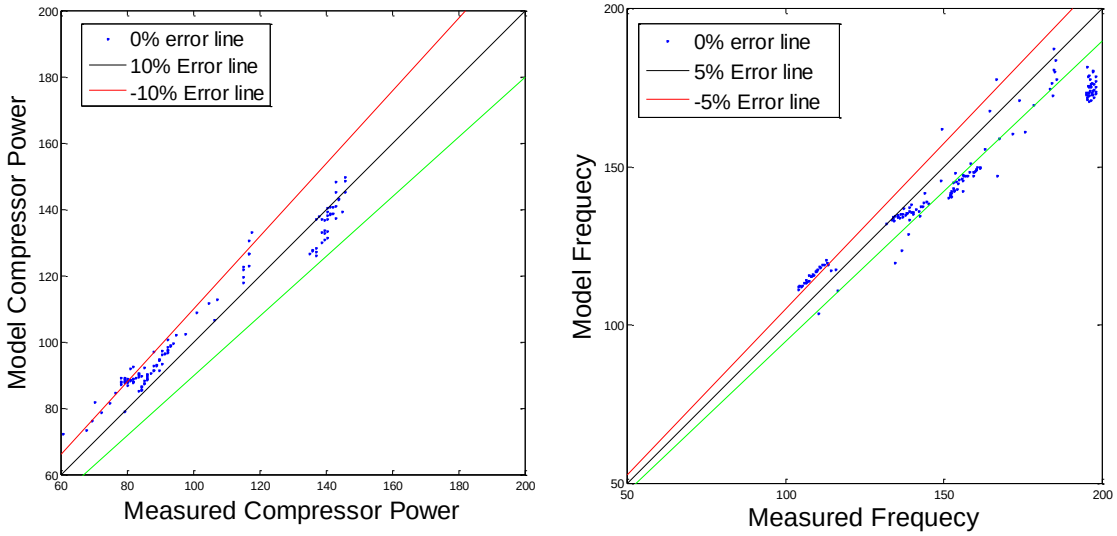

Figure 3: (a) Compressor Power Predicted vs. Measured (b) Compressor Speed Predicted vs. Measured

2.2 Heat Exchangers

For our purpose the evaporator model need only return refrigerant mass flow rate assuming negligible jacket losses and an isenthalpic throttling process at the evaporator inlet:

$$Q_e = \dot{m}_{chW} C_p \left(T_{chWrtn} - T_{chWsply}\right) = \dot{m}_{ref}\left(h_{vap,out} - h_{liq,in}\right)$$

Having resolved to model the chiller separately from the evaporator in order to reduce dimension of the boundary condition vector (Tabreed, 2013), we now focus on the condenser. The condenser model is based on Zakula's (2010) air-cooled condenser in which the refrigerant-side flow path is divided into three regions: de-superheating, condensing, and sub-cooling. Inputs to the condenser model include: refrigerant mass flow rate $\dot{m}_{ref}$, condenser air flow rate V_x, refrigerant-side inlet temperature T_{c1}, fraction of condenser devoted to sub-coolingx_{sc}, ambient temperature T_x, sub-cooling, heat transfer and pressure drop flags and condenser physical parameters
The outputs from the model are the total heat rejected, temperatures and pressures at the interface between each region, pressure drop in each region and temperature of the leaving refrigerant liquid. The total heat rejected is the sum of the heat rejected in the de-superheating, condensing, and sub-cooling condenser regions

$$Q_{c,total} = Q_{sh} + Q_{cnd} + Q_{sc}$$

Initial guesses for the condensing fraction and inlet pressure are passed to the condenser model. Based on relevant flags (pressure drop and sub-cooling) the model is initialized to account for these phenomena or to neglect them. The condenser desuperheating and subcooling sections are modeled by the crossflow effectiveness approximation:

$$\varepsilon = 1 - exp\left[\frac{\dot{C}_{max}}{\dot{C}_{min}} NTU^{0.22}\left\{\exp\left[-\frac{\dot{C}_{min}}{\dot{C}_{max}}(NTU)^{0.78}\right]-1\right\}\right]$$

where $NTU_i = U_i A_i / \dot{c}_{min}$ is the number of transfer units for the i^{th} section and $\dot{c}_{min}$, $\dot{c}_{max}$ are the thermal capacitance rates with $\dot{c}_{min}$ usually found on the refrigerant side while the air side capacitance rate is proportional to the area of the i^{th} section, A_i.

Two-phase regions are modeled by the single-stream heat-exchanger effectiveness relation:

$$\varepsilon = \left(1 - e^{-NTU}\right)$$

Heat transfer coefficients, U_i, are evaluated for each section, i, as the sum of air- and refrigerant-side resistances, obtained by standard Nusselt vs. Reynolds and Prandtl number correlations, and heat exchanger wall resistance (Zakula 2011). The fractions of total refrigerant-side surface area devoted to desuperheating and condensing are determined iteratively based on the points at which the superheated vapor reaches saturation and the vapor fraction of the condensing refrigerant reaches zero i.e. becomes 100% saturated liquid. If the fraction devoted to subcooling is specified only one area remains to be solved.

Fluid state and transport properties, including inlet and average values, for the superheated part are evaluated by NIST REFPROP. Using the NTU method, heat rejection rates in the condenser regions are evaluated in terms of the entering refrigerant temperatures, T_{ci}, by

$$Q_{sh} = \varepsilon_{sh}\dot{C}_{sh,min}\left(T_{c1} - T_x\right)$$

$$Q_{cnd} = \varepsilon_{cnd}\dot{C}_{air}\left(A_2 / A_{tot}\right)\left(T_{c2} - T_x\right)$$

$$Q_{sc} = \varepsilon_{sc}\dot{C}_{sc,min}\left(T_{c3} - T_x\right)$$

Once each state has been determined, the method checks to ensure that convergence has been met by attempting to satisfy the following equations

$$\frac{Q_c}{\epsilon_c C_c} - \left(T_{c2} - T_x\right) = 0$$

$$\frac{Q_{sh}}{\epsilon_{sh} C_{sh,min}} - \left(T_{c1} - T_x\right) = 0$$

If pressure drops and sub-cooling are included in the model, there are an additional three equations using standard correlations for pressure drop in single phase or multiphase flow. The model iterates until the verification equations are satisfied indicating that the condenser sub-model is fully converged. Condenser effectiveness is predicted within ±20% of measured effectiveness as shown in Figure 4.

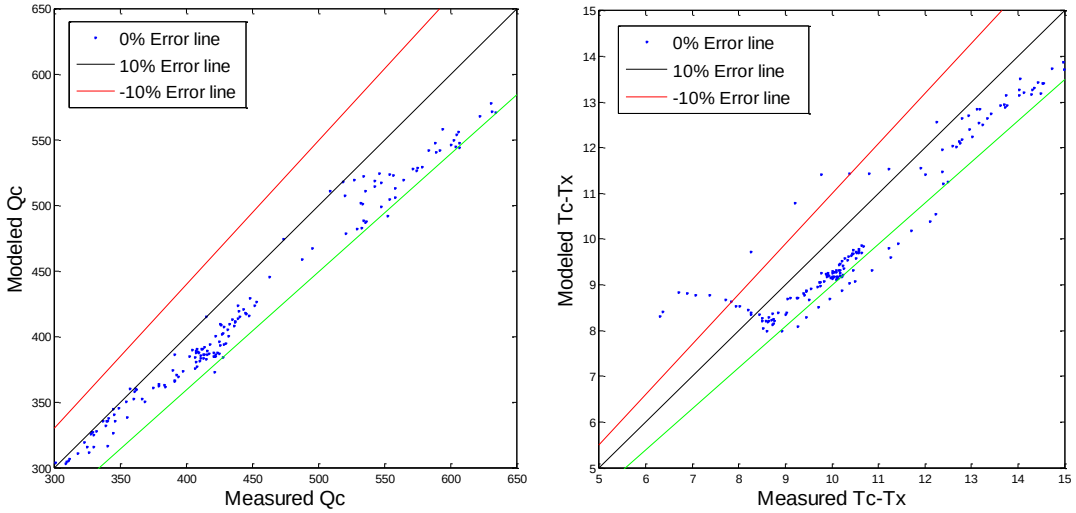

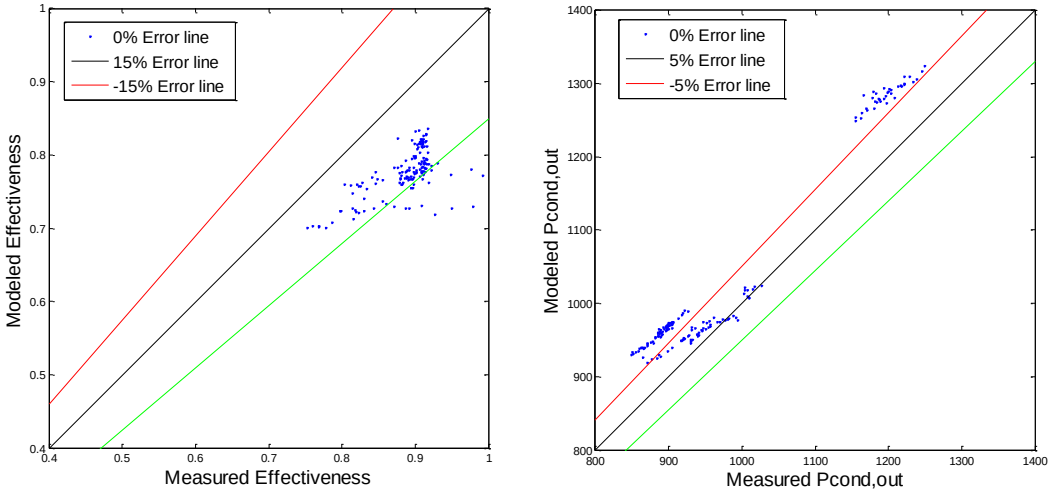

Figure 4 : Condenser: (a)Qc Predicted vs. Measured (b) Condenser outlet Temperature Predicted vs. Measured (c) effectiveness Predicted vs. Measured (d) Condenser outlet Pressure Predicted vs. Measured

3 MODELED PERFORMANCE

By decoupling the evaporator from the rest of the system we can develop performance maps of the remaining system with two refrigerant-side boundary conditions i.e. capacity and evaporating temperature, and take external air temperature as third boundary condition. Hence compressor and condenser represent a sub-system with capacity Q_e, evaporating temperature, T_e, and outdoor temperature, T_x, as boundary conditions and sub-cooling fraction, x_{sc}, as a control variable. Figure 5 maps the performance of this sub-system with ΔT_{sc} fixed at the design value of 3.4 ^{o}C. This performance map serves as the base case for design optimization. Figure 5 also shows that specific power has minimum values between 0.5-0.7 Part Load Fraction (PLF). Hence rather than operating two chillers at higher PLF (0.8 to 1.0) in summer, it may be better to operate three chillers (if available) at PLF 0.5-0.7. Figure 6 shows that for the typical range of -1<T_e<5° C performance is mainly determined by PLF and $\Delta T = T_x - T_e$.

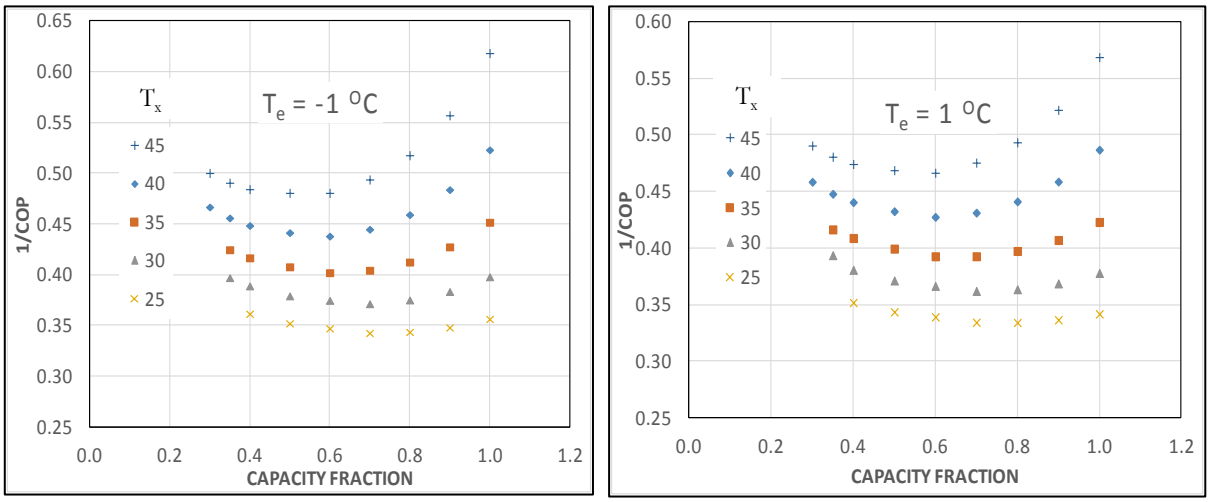

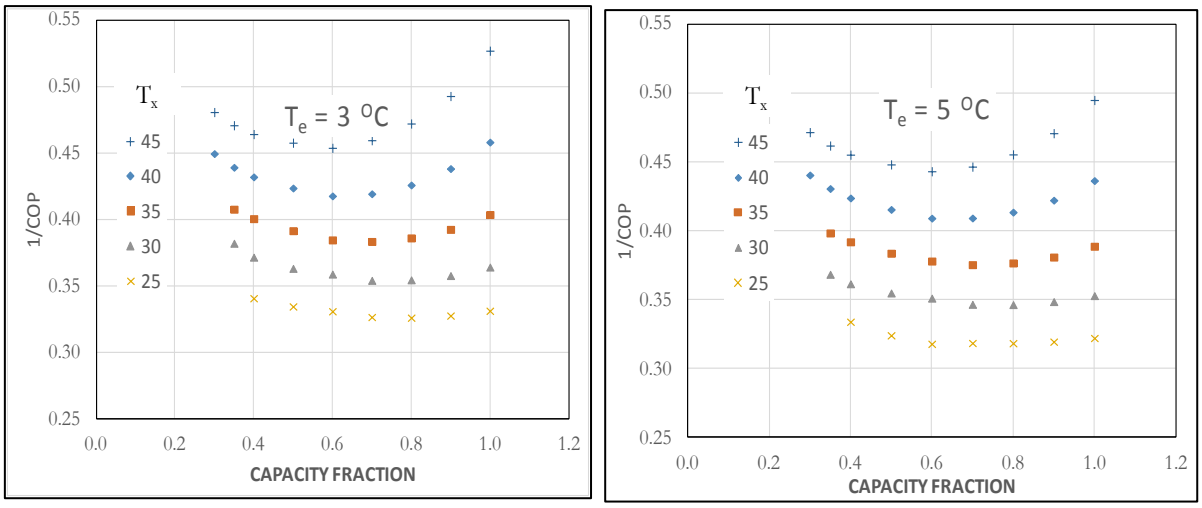

Figure 5 (a) Chiller performance over T_e = -1,1,3,5 °C and T_x = 25, 30, 35 ,40,45 °C at ΔT_{sc} = 3.4°C

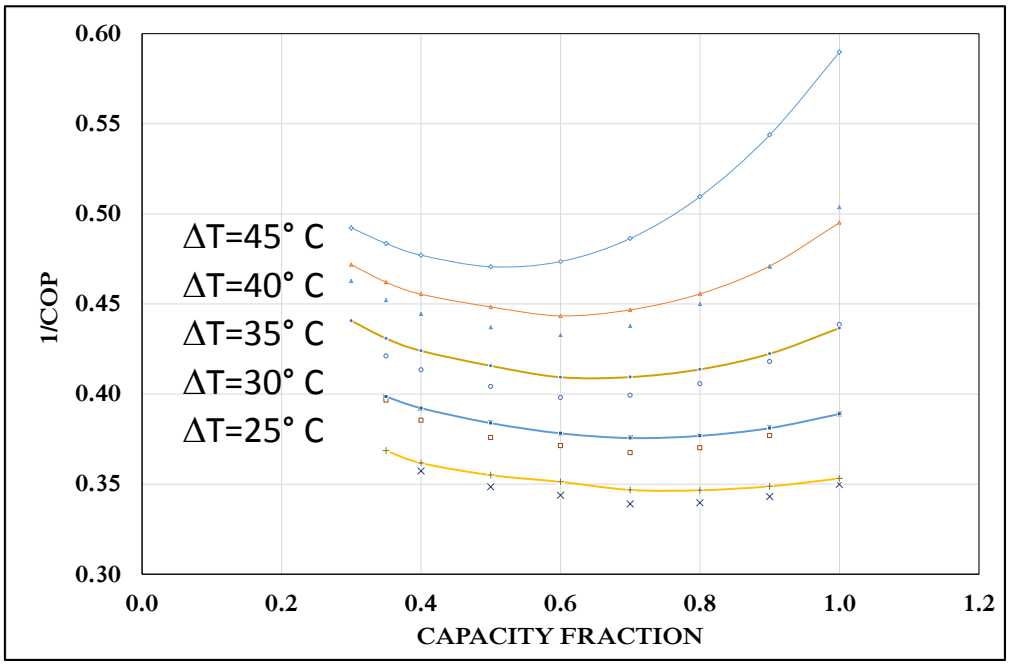

Figure 6 Chiller performance as function of capacity and external lift, $\Delta T = T_x - T_e$,

4 OPTIMIZATION AND ENERGY SAVINGS

Minimum performance standards may be established by finding chiller designs that achieve minimum life-cycle cost under regionally typical climate, electricity pricing and load profiles. In UAE the climate and cooling load profiles are among the most severe on earth. In sections 2 and 3 we have modeled and validated the performance of a baseline chiller typical of products deployed in UAE. Alternative designs may be modeled by resizing or replacing components, e.g. replacing the screw compressor by a variable speed reciprocating compressor (thus eliminating the oil separator and cooling circuit), optimizing condenser and evaporator sizes, and implementing variable speed compressor, condenser fans and optimal sub cooling controls.

High performance chiller design should encompass fully integrated design involving component design, size trade-offs, and control improvements including the following:

Component type/design and size matching:

- Compressor type including 2-stage, economized and variable-speed compressors
- Pipe size impacting pressure drop in condenser, evaporator and piping
- Heat exchanger size
- Condenser fans (variable speed)

Controls

- Variable speed compressor
- Variable speed condenser fan
- Precise evaporator superheat control
- Optimal condenser sub-cooling control

For any given combination of alternative component designs one must apply optimal control at all operating points to assess annual energy use under standard weather and load profiles. Sub cooling provides a good example. Using the same grid established for mapping chiller performance with fixed sub cooling, we run the solver within an optimizing shell to obtain optimal sub cooling at each grid point. A savings between 1-4 % is recorded with optimal (versus fixed) sub-cooling operation, shown in figure 7

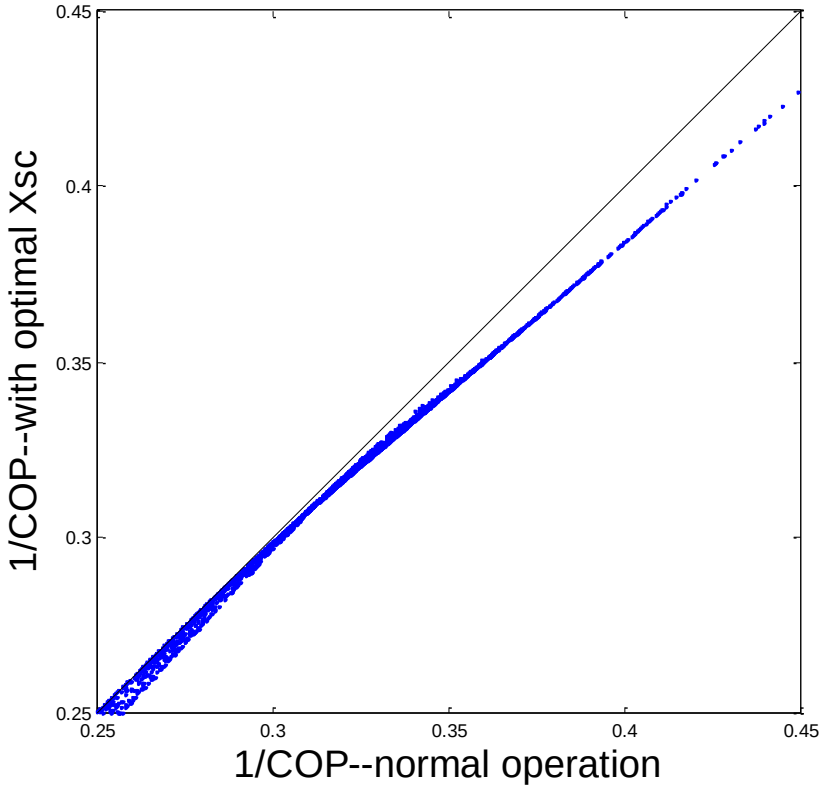

Figure 7 : Chiller mean specific power for optimal vs. fixed (3K) sub-cooling operation

The impact of a given design decision, e.g. to implement optimal subcooling control, is evaluated by hourly simulation using Abu Dhabi TMY weather, a typical weather-dependent cooling load profile (Ali 2011), and the chiller performance maps of the type generated by our model and shown in Figure 5. The Abu Dhabi daily cooling load may be used to obtain representative hourly loads (Q_C) using the weather sensitive part of the model of Ali (2011) and normalized to the peak cooling load:

$$Q_C / Q_{c,max} = C_1\left(T_x - T_0\right) + C_2\left(w - w_0\right) + C_3 DHI + C_4 DNI\cos\theta + C_5 DNI\sin\theta$$

where base temperature, T_o= 18.5°C, base specific humidity w_o = 0.0085 kg/kg, DHI = diffuse horizontal irradiation (W/m^2) DNI = direct normal irradiation (W/m^2), θ = solar zenith angle (radian), cosθ = ratio of direct irradiation on horizontal surface to DNI, sinθ = ratio of direct irradiation on vertical surface to DNI, and only the positive hourly cooling loads returned by the model are considered. Cooling plant input power is the product of hourly cooling load, Q_c, and chiller specific power, $1/COP$. Annual cooling energy use is therefore given by

$$E_c = \sum Q_c\left(T, w, DHI, DNI\right) / COP\left(T, PLR\right)$$

When cooling energy use for Abu Dhabi is evaluated by the above method for fixed and optimal subcooling controls, the annual savings for this design change alone is found to be 1.7%. Results may also be put in terms of SEER (Seasonal Energy Efficiency Ratio), a measure the efficiency of a cooling system over a standard cooling season, defined as

$$SEER = \frac{\sum Q_c\left(T, w, DHI, DNI\right)}{\sum Q_c\left(T, w, DHI, DNI\right) / COP\left(T, PLR\right)}$$

A compressor SEER value of 3.255 results for the baseline chiller as normally operated. Implementation of optimal subcooling control improved the SEER to 3.308.

5 CONCLUSION

Minimum performance standards may be established by finding chiller designs that achieve minimum life-cycle cost under regionally typical climate, electricity pricing and load profiles. In UAE the climate and cooling load profiles are among the most severe on earth. In this paper we have modeled and validated the performance of a baseline chiller typical of products deployed in UAE. Alternative designs may be modeled by resizing or replacing components, e.g. replacing a screw compressor by a variable speed reciprocating compressor (thus eliminating the oil separator and cooling circuit), optimizing condenser and evaporator sizes, and implementing variable speed compressor, condenser fans and optimal sub cooling controls. The importance of simultaneously optimizing controls with each candidate design has been illustrated for optimal subcooling.

6 ACKNOWLEDGEMENT

We thank Executive Affairs Authority (EAA) and Masdar Institute of Science and Technology for supporting this research.

7 REFERENCES

Ali, M.T., H. Javed, M. Alhamahmy, P.R. Armstrong (2014). Optimized heat pump design for GCC countries, Part II: Baseline chiller instrumentation and best practices, *Proc. 11th IEA Heat Pump Conference*

Ali, M.T., M.M. Mokhtar, M. Chiesa, P.R. Armstrong, (2011). A cooling change-point model of community-aggregate electrical load, *Energy and Buildings*, 43(1):28-37

Armstrong, P., W. Jiang, D.W. Winiarski, S. Katipamula, L.K. Norford, and R.Willingham. (2009). Efficient low-lift cooling with radiant distribution, thermal storage and variable-speed chiller controls—Part I: Component and subsystem models. *HVAC&R Research,* 15(2):367–401.

Armstrong, P, Qureshi, O.A. H. Javed (2014) *Optimal Control of a District Cooling Plant,* Tabreed Final Report.

Husseini, I.E., F. Walid, T.E. Sayed, and D. Zywietz (2008). *A New Source of Power: The Potential for Renewable Energy in the MENA Region*. Booz & Company.

Brasz, J. (2010). A proposed centrifugal refrigeration compressor rating method, *ICEC at Purdue*.

Friedrich, L.A. (2013). *An Urban Energy Baseline Model for Measurement & Verification of Building Energy Efficiency Retrofits in Abu-Dhabi*, MSESM Thesis, Masdar Institute of Science and Technology.

Hiller, C.C. and L. Glicksman (1977). Heat pump improvement using compressor flow modulation, *ASHRAE Transactions, 83(2).*

Qureshi, O.A. (2013), *Optimal Control of District Cooling System with Variable Speed Plant and Distribution*. MSME Thesis, Masdar Institute of Science and Technology, Abu Dhabi UAE.

Qureshi, O.A., H. Javed, A. Afshari and P.R. Armstrong (2014), Optimal model-based control of chiller tower fan and cooling water pump. ASHRAE 120(2).

Stoecker, W.F. and J.E. Jones (1982). *Refrigeration and Air Conditioning*, McGraw-Hill, Singapore.

Van Houte, U., & Van den Bulck, E. (1994). Modeling chiller performance using simultaneous equation-solving procedures. *International Journal of Refrigeration*, 17(3), 191-198.

Vera-García, F., J. García-Cascales, J. Gonzálvez-Maciá, R. Cabello, R. Llopis, D. Sanchez & E. Torrella (2010). "A simplified model for shell-and-tubes heat exchangers: Practical application." *Applied Thermal Engineering*, 30(10), 1231-1241.

Zakula, T., N.T. Gayeski, P.R. Armstrong and L.K. Norford (2011). "Variable-speed heat pump model for a wide range of cooling conditions and loads", *HVAC&R Research*, 17(5), 670-691.